DEVELOPMENT OF HIGH RESPONSE PRESSURE PROBES FOR TIME-RESOLVED 2D AND 3D FLOW MEASUREMENTS IN TURBOMACHINES

Dossena Vincenzo Gaetani Paolo Persico Giacomo

Dipartimento di Energetica, Politecnico di Milano, Via La Masa, 34, 20158 Milano, Italy

ABSTRACT

The unsteady flows in turbomachinery have been one of the leading research topics in the last decade. Recently, several cylindrical fast response probes both for 2D and 3D unsteady measurements have been designed and manufactured at the Politecnico di Milano.
The probes have been developed using commercial miniaturized pressure sensors encapsulated in the probe head; a line-cavity system is required and it defines the probe dynamic behaviour. Simple analytical models and unsteady numerical codes were applied to support the design of the internal geometries. Then, experimental dynamic calibrations in a low pressure shock tube were carried out: the dynamic calibration results allow to extend the probe operating range up to 80 kHz, that can be considered a suitable value for many turbomachinery applications.

NOMENCLATURE

c = sound speed in external condition
d_l = line diameter
I = amplification pick
L = line length
P = pressure
V = cavity volume
V_l = line volume
ω_n = natural frequency
ω_p = resonance frequency
ζ = non dimensional damping
μ = dynamic viscosity in external condition
ρ = density in external conditions

SUBSCRIPTS

ref = reference
t = total
s = static
m = measured
In = stage inlet

INTRODUCTION

The role of the flow unsteadiness generated by the cascades relative motion has had a growing importance in the turbomachinery research in the last decades. Starting from the works of *Giles* (1990) and *Sharma et al.* (1992) up to the latest of *Schlienger et al*. (2004), many phenomena - such as the wake rectification, the wake/boundary layer interaction, the stator/rotor secondary vortex interaction, shock wave/flow field interaction - are described and discussed.
A significant development in the experimental techniques, applied to measure unsteady phenomena, has been brought by the use of piezoresistive sensors. In some application the pressure sensors were flush mounted on the probe head, enhancing the frequency response despite to fragility and to blockage (Ainsworth et al., 1995; Miller et al., 2003). In other cases, to enhance the probe strength, the transducers were sub-surface mounted (Gossweiler et. al., 1995; Brouckaert, 2000; Barigozzi et al., 2000): as a consequence, a line-cavity system is introduced for every hole, strongly influencing the probe dynamic response. Due to the need of minimizing the probe blockage, many resources were devoted to miniaturize the sensitive elements of the pressure probes, and the smallest and most robust solution was developed installing only one sensor inside the sensitive head.
Since many years, the researchers of the Politecnico di Milano have dealt with this subject: different cylindrical single sensor fast response probes have been designed and tested (Gaetani and Persico, 2004). Design methodology, dynamic analysis and results of a first application of a cylindrical single hole fast response probe are presented and discussed in this paper.
As a future development a two sensors hemispherical fast response probe allowing for unsteady 3D measurements is described.

CYLINDRICAL PROBE CONCEPT

GENERAL SPECIFICATIONS

In general, a cylindrical one sensor pressure probe has a very low sensitivity to the flow angle in the meridional plane (pitch angle). For this reason it allows 2D flow measurements, in a plane normal to the probe axis (yaw angle), by means of three pressure values measured at different rotation angle around the probe axis. Thus the probe is operated as a "virtual three holes probe". Phase-resolved measurements can be obtained by means of a phase-locked flow reconstruction, while no direct turbulence measurements can be performed with this probe. Nevertheless some information on the turbulence intensity could be obtained by analyzing the signal acquired by the probe at the angular position aligned to the phase-averaged flow direction, if the unresolved flow angle fluctuations are sufficiently low (included in the range of ±10°)

The probe design specifications, defined according to the test rig characteristics (HP turbine stage), include:

- low blockage: external diameter < 2 mm (i.e., < 4% of the rotor blade pitch);
- frequency response of about 50 kHz (one order of magnitude greater than the rotor blades passage frequency in the nominal conditions);
- spatial resolution of the pressure tap: $d_t = 0.3$ mm

The probes were developed using commercial miniaturized pressure sensors (Kulite XCQ-062, FS = 25 Psi, temperature compensated); this approach assures high reliability, low costs and simplifies the probe heads manufacturing. Since the sensor is already mounted in a 10-30 mm long shield, it is necessary to install the sensor axially inside the probe head leading to a minimum probe head diameter of 1.8 mm. So operating the final spatial resolution of the probes, defined as the physical distance between the extreme positions of the tap during the three rotations, is 1.4 mm.

STEADY AERODYNAMIC CALIBRATION

The probes steady aerodynamic tests were performed on a calibrated nozzle supplied by air. The calibration procedure and the 2D flow field reconstruction in terms of total and static pressure, yaw angle and Mach number, requires the definition of three calibration coefficients:

$$K_{pt} = \frac{\left(P_{t,ref} - P_c\right)}{\left(P_t - P_s\right)_{ref}} \quad K_{ps} = \frac{\left[P_{s,ref} - (P_l + P_r)/2\right]}{\left(P_t - P_s\right)_{ref}}$$

$$K_{yaw} = \frac{\left(P_l - P_r\right)}{\left(P_t - P_s\right)_{ref}}$$

where P_c is the maximum (central) pressure measurement among the set of acquired ones, while P_l and P_r are respectively the one on the left and on the right of P_c. The angular step between the different pressure measurements is 45°, resulting in a calibration range of ± 22.5°. Due to the chosen angular step, a maximum of eight angular positions are required when the average flow direction is unknown on 360°.

The steady calibration was verified on the same nozzle, at several Mach number and yaw angle, giving the maximum errors reported in table 1. The error e is defined as the difference between the measured and the expected known quantity:

$$e = X_m - X_{ref} \qquad (1)$$

X	$P_t / (P_t - P_s)_{ref}$	$P_s / (P_t - P_s)_{ref}$	*Yaw*
e	± 0.5 %	± 0.5 %	± 0.5 °

Table 1: Maximum measurement errors

It has to be noted that the errors in tab. 1 take into account the sensor static accuracy (80 Pa), the thermal drift affecting the miniaturized sensor and the interpolation between coefficients at different calibration Mach numbers.

EXPERIMENTAL TOOL FOR DYNAMIC CALIBRATION

Due to the high blade passage frequency of the test rig where the probe will be applied, the constraint on the probe frequency response is the most important. The preliminary analyses on the first manufactured probe (Barigozzi *et. al.*, 2000) demonstrated that the dynamic calibration facility characteristics were not suitable for the design specification. For these reasons, an experimental facility was expressly developed for the dynamic calibration by means of the experimental step response.

SHOCK TUBE CHARACTERISTICS

Since a pressure signal frequency content up to 100 kHz is required, an open end shock tube has been designed and developed (Gaetani and Persico, 2003). The facility is 6.5 m long and it has a diameter of 80 mm; at the diaphragm burst, a weak shock wave of 0.3 bar is generated. Due to the low pressure acting in the diaphragm burst process, a partial opening occurs (typically the maximum opened diameter is 75% of the tube internal diameter), reached after 400 µs. As a consequence of the partial opening a diffracted shock (or compression) wave is generated immediately past the diaphragm burst. The reflection of the curved parts of the diffracted wave on the walls and on the tube axis generates pressure fluctuations on the plateau following the shock wave. The pressure oscillation frequencies range from 5 kHz to 15 kHz, and are within the region of interest for the dynamic calibration; anyway the pressure fluctuations amplitude decreases as the distance from the diaphragm increases. For these reasons a key feature of the facility is the distance between the calibration section and the diaphragm: after several experimental and numerical analyses a distance of about 3 m was chosen. A typical reference signal, acquired by means of a miniaturized flush mounted total pressure probe located at the tube axis, and its amplitude spectrum are shown in figure 1.

As it can be seen, the pressure oscillations on the plateau (of about 7 ms of duration) are still present also in the calibration section, and they may act as

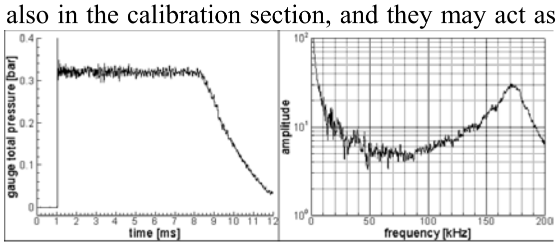

Figure 1: typical reference signal and its amplitude spectrum at the calibration section

a noise in the transfer function evaluation.

A methodology that eliminates the effects of the pressure fluctuation will be discussed in the following. In this way a complete dynamic analysis (i.e., system parameters identification) will be possible.

SHOCK TUBE FIRST APPLICATION

At first the shock tube was used in order to verify the dynamic behaviour of the probe presented in *Barigozzi et al.* (2000), called CYL-1 in the following. The CYL-1 internal geometry is characterized by a cylindrical cavity with a base diameter of 1.4 mm and a height of 0.3 mm, equal to the line diameter; thus the line length is 0.2 mm. The volume geometry was designed to guarantee a full sensor membrane stress. The dynamic analysis results are reported in figure 2, where the response signal points out a behaviour of an over-damped second order system, characterised by a 5% settling time (defined as the time required to reach the 95% of the stimulus step signal) of nearly 57 μs. Moreover strong oscillations are clearly visible in the signal. The spectrum (not shown for sake of brevity) has a high frequency pick at 240 kHz: this feature, corresponding to the signal oscillation, is related to the acoustic waves propagation inside of the cavity. The comparison with the reference signal spectrum (Gaetani and Persico, 2004) suggests an application range limited at 10 kHz, in agreement with the previous analyses.

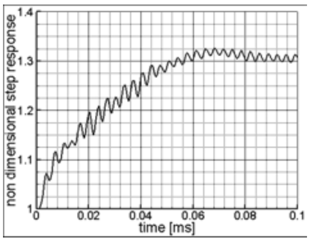

Figure 2: CYL-1 experimental step response

ENHANCING OF DYNAMIC PROPERTIES

While external miniaturization is limited by the transducer dimensions, the design of the probe internal cavities undergoes to less constrains. Thus resources were dedicated to the internal geometry miniaturization in order to improve the dynamic response.

In the following section the geometry of the new probe, called CYL-2, together with the dynamic behaviour is described. The design methodology was based on manufacturing skills, simple analytical models and numerical simulations.

PROBE INTERNAL GEOMETRY

The CYL-2 probe geometry is presented in figure 3. The line-cavity system is characterised by a conical volume (base diameter = 0.8 mm and height = 0.3 mm), and by a cylindrical line (diameter = 0.3 mm and length about 0.7 mm). The conical shape was chosen in order to reduce the volume. The cavity has been designed to guarantee a partial sensor membrane stress, roughly corresponding to the piezoresistive elements position on the membrane, even if a lower sensitivity is expected.

Once the shape of the CYL-2 internal geometries was chosen, a preliminary analysis was carried out by means of analytical models in order to refine the design.

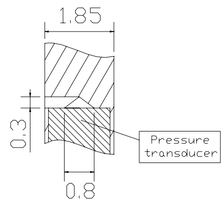

Figure 3: CYL-2 head geometry

Unfortunately, all the models work under heavy hypothesis such as the assumption of linearity in the line-cavity system behaviour. In fact the non linearity of the empting and filling process and of the effects of turbulence, is intrinsic in this measurement technique and have to be taken into account in its applications. The other principal hypothesis are:

- axial volume length negligible with respect to the line length: this allows to consider the fluid motionless (but compressible) in the cavity.
- line volume negligible with respect to the cavity volume: this allows to consider incompressible the flow within the line.
- wave propagation neglected in the line-cavity system.
- laminar flow in the line (for the linearity), while in the cavity there is no motion and thus no viscous effects can be introduced.

Moreover a concentrate parameters analysis cannot consider geometrical details such as the line axis orientation with respect to the cavity and the cavity shape.

Anyway the model proposed in Doebelin (1990) appears to be very suitable for the CYL-2 geometry: it takes into account the compressibility effects in the line, and it introduces a correction for small line lengths with respect to the line diameter. The following expressions for the line-cavity system natural frequency (ω_n) and non-dimensional damping (ζ), applied to the geometry reported in figure 3, give:

$$\omega_n = \frac{c}{\left(L + \frac{8}{3\pi} d_l\right)\sqrt{\frac{1}{2} + \frac{V}{V_l}}} \cong 47 kHz$$

$$\zeta = \frac{16\mu\left(L + \frac{8}{3\pi} d_l\right)}{d_l^2 c\rho} \sqrt{\frac{1}{2} + \frac{V}{V_l}} \cong 0.013$$

The estimated natural frequency is similar to the one required by the design specifications; the very low damping predicted by the model appears not to be significative because the viscous effects, the waves propagation and the sensor position, governing the system damping, cannot be properly captured.

STEP RESPONSE & TRANSFER FUNCTION

The encouraging results obtained by the theoretical analysis (confirmed by CFD simulation) brought to manufacture the CYL-2 probe according to figure 3. The probe was tested in the shock tube and the experimental step response is presented in figure 4. The experimental signal shows a dynamic typical of an under-damped second order linear system, characterized by heavy over-elongations at a constant frequency, roughly equal to 50 kHz. The strong oscillations at 240 kHz that characterized the CYL-1 behaviour are not visible in the CYL-2 step response, probably because the cavity conical shape tends to bare the acoustic propagation, leading to a more uniform pressure distribution in the cavity and reducing the response time.

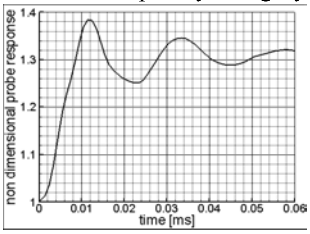

Figure 4: CYL-2 experimental step response

In order to quantify the dynamic properties of the instrument and to dynamically correct the data in the application, the probe experimental transfer function was calculated.

In general the transfer function is defined as the complex ratio between the probe and the reference signals Fourier transforms: thus, it requires the acquisition of the reference signal, and it may be evaluated in different ways. At first, a rough calculation can be derived directly from the whole signals. For a shock tube calibration this approach would introduce in the transfer function calculation not only the electrical and mechanical disturbances, but also the effects of the pressure oscillations in the reference signal (between 5 kHz and 15 kHz) and the resonance of the reference transducer (over 40 kHz).

In the present paper, a different methodology is proposed: since the shock is fully developed in the measuring station, the reference signal is only used to trigger a theoretical pressure step of the same amplitude (without losing, in this way, the phase information); the probe signal is considered only for the period necessary to complete its dynamic response, without any smoothing or filtering operation.

A transfer function analysis has allowed to quantify the dynamic performances of the CYL-2 probe: the amplitude and phase diagrams are shown in figure 5.

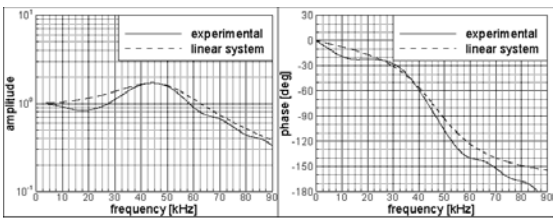

Figure 5: CYL-2 probe experimental and linear transfer function

The amplitude diagram pick, at a frequency of 44.2 kHz, represents the line-cavity system resonance and the amplification pick (I = 1.71), provides an estimation of the non dimensional damping. Using the following relations, we obtain:

$$I = \frac{1}{2\zeta\sqrt{1-\zeta^2}} \Rightarrow \zeta = 0.306$$

$$\omega_p = \omega_n\sqrt{1-\zeta^2} \Rightarrow \omega_n = 49.1 \ \ kHz$$

The analytical linear transfer function charcterized by these parameters is also plotted in figure 5, in order to evaluate the role of the non-linear effects on the probe dynamic behaviour. With respect to the linear amplitude, a slight de-amplification can be seen in the frequency range between 5 kHz and 35 kHz, but the amplitude never undergoes the value of 0.8. For higher frequencies, up to 90 kHz, the displacement from the linear amplitude becomes evanescent. The phase diagram shows a higher absolute phase displacement for low frequencies with respect to the whole range (up to 25 kHz) and a good linearity up to 80 kHz. In this frequency range, the maximum difference between the experimental and theoretical phase diagrams is always lower than 20°; moreover, the natural frequency deduced by the experiment (corresponding to the frequency for -90° of phase displacement) is about 47 kHz and differs of 4% from the linear one. It must be underlined that the pressure step level is of the same order of the maximum fluctuations intensity expected in the turbine stage experimental application; thus, this represents the worst condition for the probe linearity, and for normal operating conditions (i.e., lower fluctuation intensity) even a better linearity is expected.

The frequency analysis shows that the CYL-2 probe is very suitable for the test rig application evidencing a high resonance frequency, that is in good agreement with what was predicted by the analytical estimate (less than 10% as error). The validity of the model (at least for the resonance frequency) allows to correct the transfer function in order to consider the sound speed difference between the shock tube and the turbine test rig.

Moreover, since the low resonance pick amplitude, the application range could be extended over the resonance frequency and, by means of numerical compensation, the CYL-2 probe can be considered suitable to capture signals with harmonic content up to 80 kHz.

PROBE APPLICATION IN THE TEST RIG

Once the aerodynamic and dynamic calibration has been completed, the probe was applied downstream of the rotor of an HP gas turbine installed in the closed loop test rig for Compressors and Turbines located at the Politecnico of Milan. A detailed description of the test rig is reported in *Gaetani et al. 2004*. The operating condition are an expansion ratio of 1.35 and a rotor blade passage frequency of 2.83 kHz; the rotor tip diameter is 0.4 m and the blade height is 50 mm.

The probe position is fixed with respect to the casing while the stator can be moved.

In the preliminary measurements here reported the probe was at 0.4 axial rotor chord downstream the rotor trailing edge and at midspan. The pressure signal was acquired at 1 MHz for 1 second in order to have a great amount of data and to allow a statistical analysis of them. Since no information on the unsteady flow field direction was available before of this measurements campaign, a set of 7 probe rotation was scheduled; the data acquired at each probe rotation were then phase-averaged in 40 points each rotor pitch for the whole rotor revolution (i.e. 1000 points on a rotor revolution). At each point, the three pressure values (P_c, P_l, P_r) among the 7 acquired were chosen and the unsteady flow field, in terms of pressure, velocity and yaw angle, was computed.

This procedure was repeated for each stator tangential position, leading to the phase-rotor to phase-stator map afterward reported.

In order to quantify the unsteady measurements reliability, they were time-averaged and compared with the ones obtained by a miniaturised five hole pressure probe. The standard differences σ defined as:

$$\sigma = \sqrt{\frac{\sum_i e_i^2}{N-2}} \quad \text{where} \quad e = X_{unst} - X_{5hole}$$

are reported in table 2 in terms of :

X	Cp_t	Cp_s	Mach Number	Yaw
σ	0.01	0.02	0.015	3°

Table 2: standard differences between 5hole probe data and time-averaged data by unsteady probe

where Cpt and Cps are defined according to:

$$C_{px} = \frac{P_x - P_{ref}}{P_{t,in} - P_{ref}}$$

The differences between the time-averaged measurements derived by the two probe arise from the thermal drift affecting the fast response probe and from the non perfect repeatability of the operating condition in terms of total temperature and expansion ratio. Regarding thermal drift, the sensor installed inside the probe is temperature compensated but no temperature calibration has been made; anyway this problem affect only the DC component of the signal, while the AC component is resolved by the aerodynamic calibration accuracy.

DYNAMIC ANALYSIS

In order to evaluate the frequency content of the pressure signal, a FFT on the raw data acquired has been computed. The results, reported in figure 6, evidence a considerable frequency content up to 20 kHz; moreover the first six rotor blade passage harmonics are clearly visible but only the first and the second ones have a meaningful amplitude. There are two more harmonics at 3.3 kHz and 6.2 kHz, not in phase with the rotor blade frequency: the first is related to the blade passage frequency of the centrifugal compressor that drives the test rig (also its second harmonics is still present). The second harmonic at 6.3 kHz may be related to the rotor trailing edge vortex shedding that causes,

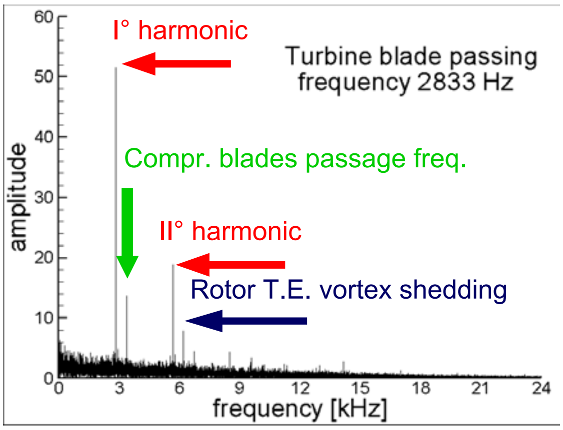

Figure 6: FFT analysis on raw pressure data

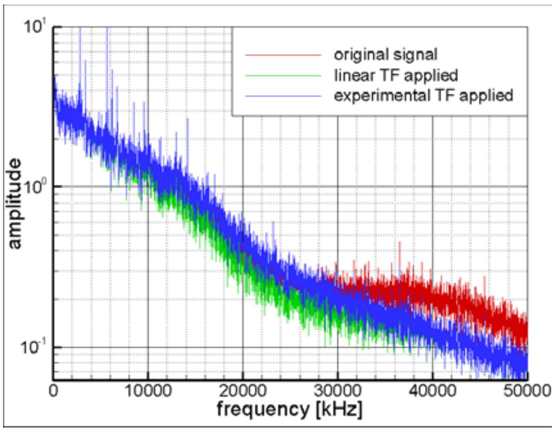

Figure 7: pressure signal amplitude spectra - comparison of transfer functons application

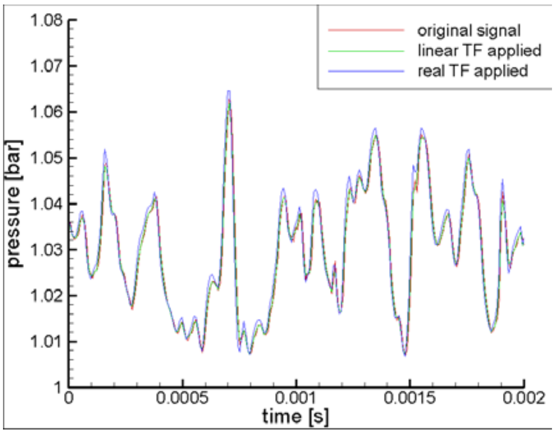

Figure 8: pressure signal before and after the transfer function application

primarily, a yaw angle fluctuation seen by the probe as pressure fluctuation.

Transfer function application: despite the raw pressure signal frequency content is included in the range of 20 kHz and that this range is very far from the line-cavity system resonance (about 1/3), the transfer function has been applied in order to verify its effects on the signal and to quantify the non linearity of the real system dynamic behaviour.

In figure 7 the effect of the transfer function on the signal spectrum amplitude can be observed: first of all, the plotting in a logarithmic scale put in evidence that a small excitation corresponding to the system resonance exists in the original signal. Applying the transfer function (experimental or linear) this amplification can be corrected, obtaining a more physical decreasing trend. This fact appears to confirm the good linearity of the line-cavity system dynamics, at least around its resonance frequency.

The effects of non linearity between 10 kHz and 35 kHz can also be noted, in terms of amplitude spectrum displacement: in this region the correction given by the experimental transfer function appears to lead to a more realistic spectrum, but further analyses on this topic are required. Anyway since the energy related to this frequencies is very poor, the uncertainties induced by the non linearity of the probe dynamic behaviour play a marginal role with respect to other sources of error. This fact is proved by the comparison of the original pressure signal with the ones obtained after the application of the transfer functions, showed in figure 8. Some differences can be noted only in correspondence of the picks, but disagreements are of the same order of the sensor expanded uncertainty.

Phase-Resolved Measurements: once the raw pressure signal is phase-locked and phase-averaged, its frequency content is modified; the harmonics not in phase with the rotor blade passage, such as the rotor trailing edge vortex shedding or the centrifugal compressor blade passage frequency, are lost.

Phase-resolved flow field measurements at midspan for different stator positions are reported in figure 9: it has to be recalled that in this representation the rotor effects are parallel to the abscissa, since the probe is always at the same distance with respect to the key phasor and then to the rotor blade. On the contrary, stator effects are parallel to the vertical axis since they are not dependent on the rotor revolution.

As showed in figure 9a-b, there is a correspondence between the yaw positive regions and the total pressure minimum: a positive yaw angle evidences a flow in the same direction of the peripheral speed and then a zone characterised by a

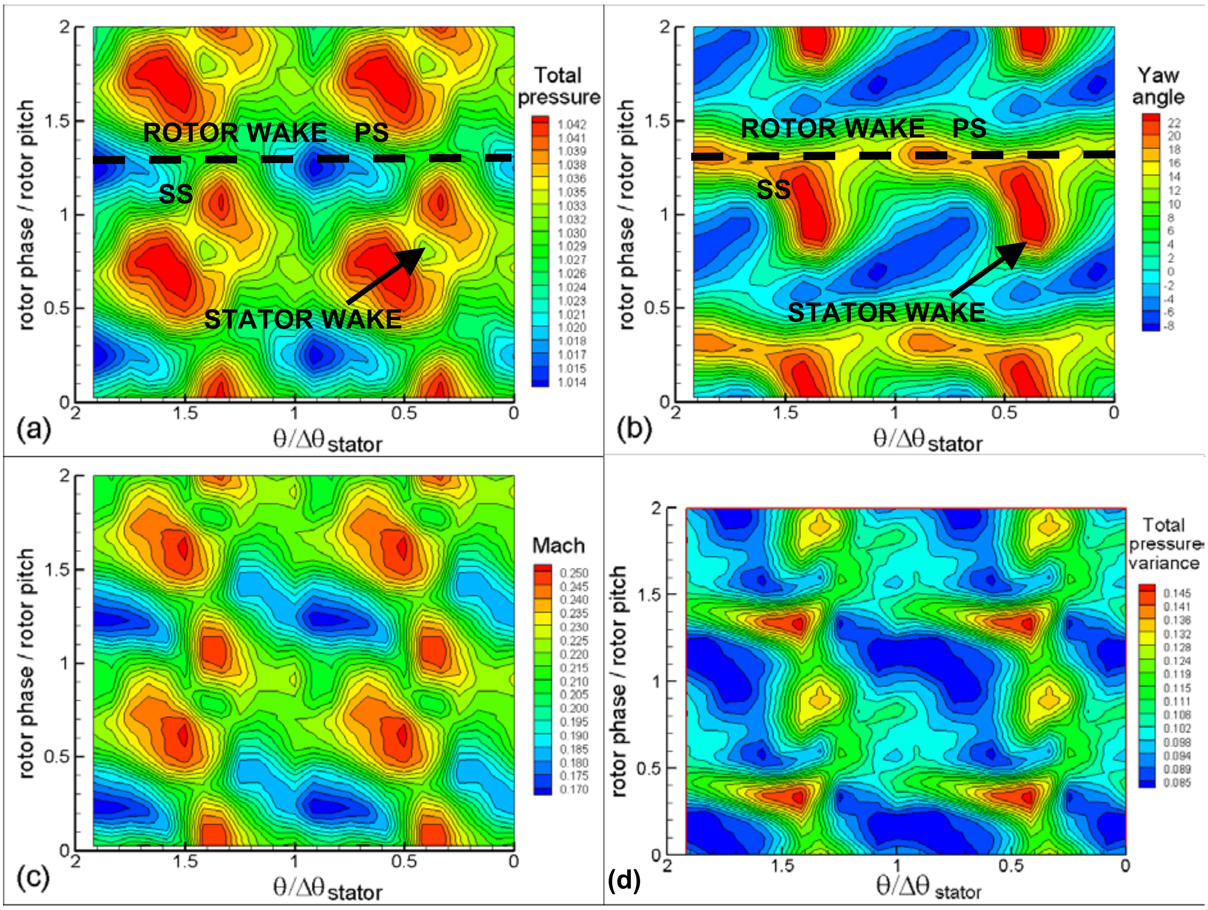

Figure 9: Phase-resolved flow field downstream the rotor as a function of the non-dimensional stator pitch

low work extraction. This feature is related to the low momentum fluid belonging to dissipative phenomena such as the stator or the rotor wake. To this flow feature is related a low total pressure level evidencing high losses occurred on those streamline.

Figure 9 shows both rotor and stator wake. In particular the rotor wake appears as a region at about the 30% of the rotor pitch along the whole stator pitch characterised by a high yaw angle level; the local yaw angle value in the rotor wake depends on the stator-rotor interaction, that will not be discussed in the present paper. Rotor suction and pressure side can be identified by geometrical consideration on the stage and on probe position.

As well known, due to the transversal pressure gradient in the rotor channel, the stator wake, during its transport in the rotor channel, is convected towards the rotor suction side. As discussed in *Gaetani et al. 2004*, where time-average pressure and temperature measurement downstream the rotor are presented, the stator wake is located at about the 45% of the stator pitch. By combining the above reported consideration, the stator wake can be evidenced as the high yaw angle and low total pressure region located at about 45% of stator pitch and 80 % of the rotor pitch.

The Mach number map, very similar to the total pressure one, confirms the almost constant static pressure level at midspan.

Figure 9d shows the Variance of the pressure signal acquired at the probe yaw angle equal to zero with respect to the axial direction: since the phase-averaged flow is almost within the range of low sensitivity of a total pressure probe, such a pressure signal can be considered similar to a total pressure one. The map shows high level of variance and then a raw estimate of the total pressure unsteadiness, exactly in the same position of the rotor and the stator wakes, confirming the flow pattern above described.

HEMISPHERICAL PROBE

Since unsteady turbomachinery flows are intrinsically three dimensional, a fast response probe suitable for unsteady 3D measurements was designed and tested at the LFM.

The probe operating mechanism is still based on multiple pressure readings taken at different rotations of the probe around its own stem: the combined use of four pressure readings allows the definition of the 3D flow field, by means of a set of previously defined calibration coefficients.

PROBE HEAD GEOMETRY

On the basis of the consolidated philosophy of CYL-1 and CYL-2, also the new probe design is based on the use of two commercial pressure sensors located inside of the probe head: this feature obviously leads to a higher diameter of the probe with respect to the previously presented cylindrical probes.

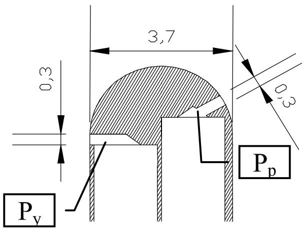

Figure 10: Hemispherical probe head geometry

The new probe head has an hemispherical shape instrumented with two pressure taps (figure 10): the first one is located on the equatorial plane, while the second one is located on the spherical surface. The second pressure tap (P_p), only used for the evaluation of the pitch angle, presents an angle of 30° with respect to the equatorial plane. Moreover, pressure tap P_p is located at 180° with respect to the P_y tap around the probe stem.

The final head geometry, representing a compromise between probe pitch sensitivity, probe head dimension minimization and frequency response, leads to an head diameter of 3.7 mm and to a diameter of 0.3 mm of the two pneumatic lines feeding the cavities facing the two pressure sensor membranes.

The pneumatic line P_y geometry is identical to the one of CYL-2, while the line P_p is shorter and inclined with respect to the sensor membrane: this features influence the probe response, as it will shown in the following.

AERODYNAMIC CALIBRATION

The calibration process is similar to the one described for the single hole cylindrical probes: the hemispherical probe can be still operated as a "virtual multi-hole probe", requiring:

- three pressure readings at three rotation angles for tap P_y (P_l, P_c, P_r)
- one reading of pressure P_p, taken when P_p tap is located at the same angular position of P_c (central reading for P_y)

Thus an angular interval of 45° can still be used for the definition of the calibration coefficients; thus a yaw calibration range of ±22.5° with respect to the incident flow can still be assumed.

As previously mentioned, pressure reading P_p is

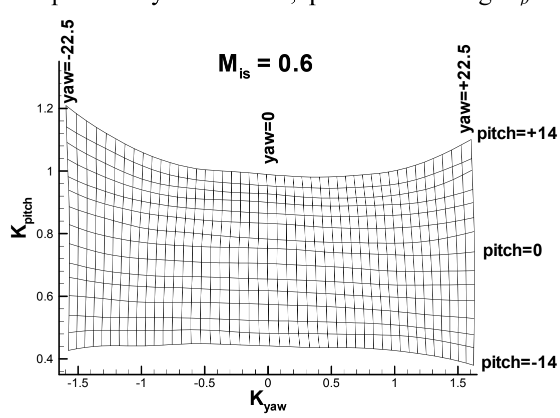

Figure 11: K_{yaw} versus K_{pitch} distribution at a calibration Mach number of 0.6.

only used for the evaluation of the pitch sensitivity coefficient K_{pitch}, while the K_{yaw} coefficient maintains a definition very similar to the one used for the cylindrical probe:

$$K_{pitch} = \frac{(P_c - P_p)}{(P_{max} - P_s)} \qquad K_{yaw} = \frac{(P_l - P_r)}{(P_{max} - P_s)}$$

where P_{max} is evaluated as the maximum of the parabola passing for P_l, P_c and P_r.

The use of P_p leads to the fact that the two angular coefficients - that are a function of yaw angle, pitch angle and Mach number - result to be slightly cross-correlated. This fact is evidenced by the quasi-perpendicular and very regular distribution of the K_{pitch} vs K_{yaw} lines plotted at constant pitch and constant yaw in figure 11.

The other two coefficients K_{ps} and K_{pt} maintain the same definition given for the cylindrical probe.

ACCURACY AT STEADY STATE

The definition of the four unknown flow parameters (yaw and pitch angle, total and static pressure) is obtained by means of the application of an iterative algorithm based on the calibration coefficient set.

In order to evaluate the hemispherical probe accuracy, the probe have been placed in the calibration jet for a large number of different combination of known yaw angle, pitch angle and Mach number. The calibration coefficients were previously evaluated in a range defined by:

- Yaw angle : ± 22.5° (step 2°)
- Pitch angle : ± 14° (step 2°)
- Mach number: 0.2 – 0.6 (step 0.1)

In order to give an example of the measurement methodology accuracy, figure 12 shows the isolines of measurement error, defined according to eq. (1), on the whole angular calibration range for a Mach number of 0.4, and obtained by means of 240 measurement points. Figure 12 shows that:

- the yaw angle is captured with a general accuracy level lower then 0.1° evidencing a maximum error of 0.2°.

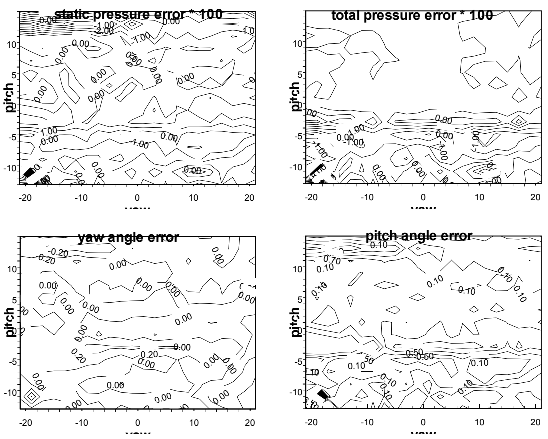

Figure 12: iso-lines of measurement errors at Mach number = 0.4

- the pitch angle error shows a maximum value of 0.8° and a general level lower than 0.5°.
- Total pressure error is lower than 1% for all the tested range.
- The static pressure error is generally lower than 1%, except at higher pitch angles (2%).

When the probe is applied at intermediate Mach number with respect to the calibration ones, the pick errors rise up to 1.5 degree and to 1 degree in the evaluation of pitch and yaw angle. The lack in angular accuracy leads to pick errors of 4.5% in the evaluation of total and static pressure.

Table 3 reports the value of the standard error σ, evaluated on 1631 measuring points taken on the whole angular and Mach number calibration range.

X	Yaw [deg.]	Pitch [deg.]	Pt / (Pt -Ps) (%)	Ps / (Pt - Ps) (%)
σ	0.20	0.71	0.96	1.30

Table 3: standard error σ on the whole calibration range for the hemispherical probe

DYNAMIC CALIBRATION

Once the aerodynamic calibration was completed, the dynamic behaviour of the probe was analysed with the same methodology used for cylindrical probes. As a preliminary consideration the dynamics is extremely important for this kind of probe, because only an high frequency response in the pitch angle measurement can justify the complications on the probe head aerodynamics.

First of all, the P_y line-cavity system has the same geometry of the CYL-2 and then it has the same dynamic properties.

The line-cavity system of the P_p pressure tap was designed on the basis of the former ones: a conical cavity with the same dimensions of the one in the CYL-2 system is connected to the tap by a line of 0.3 mm as diameter. The main difference with respect to the other systems is the angle of 60° between the axis of the line and the axis of the cavity: as a consequence the line length is reduced and the acoustic waves propagation is modified.

The first effect can be quantified by means of the analytical model before discussed, that suggests a natural frequency (ω_n) of 52 kHz. Despite the accuracy of the model, the damping estimate is still inaccurate and the effect of the shape of the system cannot be properly modelled.

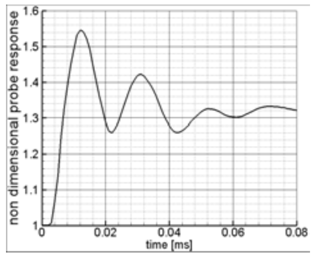

Figure 13 : P_p tap experimental step response

The probe was then tested in the shock tube and the experimental step response of the P_p line-cavity system is shown in figure 13. The signal shows the typical trend of a second order linear system, with severe overshoots at nearly constant period of about *20 μs*. Even if the resonance frequency appears to be very similar to the CYL-2 one, the P_p step response is characterized by stronger overshoots.

The system experimental transfer function was determined and it is presented in figure 14. On the basis of the amplitude pick the system was identified according to a second order linear system (the resulting linear transfer function is also plotted in figure 14), obtaining ω_n = 49.9 kHz and ζ = 0.1648.

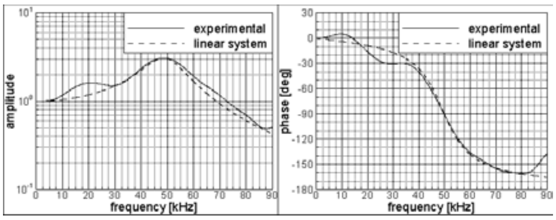

Figure 14: CIL-2 probe experimental and linear transfer function

With respect to the CYL-2 (or P_y) system the resonance frequency is very similar but the non dimensional damping is 0.5 times the former. This behaviour is probably due to the different inclination of the line in the two systems: the acoustic waves front has a component normal to the base of the cone (and thus to the transducer's membrane) and this probably strengthen the empting and filling process inside the cavity.

Considering now the comparison with the linear system, a very good linearity can be observed in the frequency range between 30 kHz and 80 kHz, while in the region between 5 kHz and 30 kHz there are some differences either in amplitude and phase that can be taken in account in the probe application by means of the use of the experimental transfer function.

Since the P_p system has dynamic performances similar to the P_y one, the hemispherical two-holes probe allows 3D phase-resolved measurements up to 80 kHz.

CONCLUSION

The development of design methodology of fast response probes was presented. A new cylindrical single sensor probe, characterised by a line-cavity system resonance frequency of 50 kHz, was designed and tested. The probe experimental transfer function, obtained by a dynamic calibration in a shock tube, allows to extend the frequency application range up to 80 kHz.

The probe was applied downstream a HP turbine stage: the transfer function application were discussed and an unsteady flowfield analysis was carried out. The comparison of the time-averaged measurements with 5-hole probe data shows some differences, due to transducer thermal drift.

Finally a two-hole probe for unsteady 3D measurements was designed and tested, evidencing 80 kHz as frequency response and low standard errors, even if affords has to be devoted to reduce the maximum errors.

REFERENCES

Doebelin E.O.,1990, Measurement System, Application and Design, McGraw-Hill Publishing Company

Giles M. B., 1990, "Stator/Rotor Interaction in a Transonic Turbine", Journal of Propulsion and Power, vol 6, pag 621

Sharma O. P., Pickett G. F., Ni R. H., 1992, "Assesment of Unsteady Flows in Turbomachinery", ASME Journal of Turbomachinery, vol. 114 pag. 79-90

Gossweiler C., Kupferschmied P., Gyamarthy G., 1995, “On Fast- Response Probe, Part 1: Technology, Calibration and Application to Turbomachinery”, ASME Journal of Turbomachinery, Vol. 117/4, pag. 611.

Ainsworth R.W., Allen J.L., Batt J.J.M., 1995, "The Development of Fast Response Aerodynamic Probes for Flow Measurements in Turbomachinery", ASME Journal of Turbomachinery, Vol. 117/4, pag 625.

Brouckaert J.F., 2000, “Development of single hole and Multi-hole fast response pressure probes for turbomachinery application” 15th Symposium on Measuring Techniques for Transonic and Supersonic Flows in Cascades and Turbomachines., Firenze

Barigozzi G., Dossena V., Gaetani P., 2000, “Development and first application of a single hole fast response pressure probe” 15th Symposium on Measuring Techniques for Transonic and Supersonic Flows in Cascades and Turbomachines., Firenze.

Miller R. J., Moss R. W., Ainsworth R. W., Horwood C. K., 2003, "Time-Resolved Vane-Rotor Interaction in a High-Pressure Turbine Stage", ASME Journal of Turbomachinery, vol 125, pag. 1-13

Gaetani P., Persico G., 2003, “Progettazione, realizzazione e caratterizzazione di un tubo d’urto per taratura dinamica di sonde di pressione”(Design, realization and characterization of a shock tube for dynamic calibration of pressure probes), 58° congresso ATI, San Martino di Castrozza (I)

Gaetani P., Persico G., 2004, “On the development of cylindrical fast response pressure probes” 59° Congresso ATI, Genova (I)

Gaetani P., Osnaghi C. and Persico G., 2004, "Preliminary analysis of stator-rotor interaction in a high pressure turbine stage", 59° Congresso ATI, Genova (I)

Schlienger J., Kalfas A.I., Abhari R.S., 2004, “Vortex-wake-Blade interaction in a Shrouded Axial Turbine” Asme paper GT2004-53915.